Article

Electrospun Poly(lactide-*co*-glycolide-*co*-3(*S*)-methyl-morpholine-2,5-dione) Nanofibrous Scaffolds for Tissue Engineering

Yakai Feng [1,2,3], Wei Lu [1], Xiangkui Ren [1,2,*], Wen Liu [1], Mengyang Guo [1], Ihsan Ullah [1] and Wencheng Zhang [4,*]

[1] School of Chemical Engineering and Technology, Collaborative Innovation Center of Chemical Science and Chemical Engineering, Tianjin University, Tianjin 300072, China; yakaifeng@tju.edu.cn (Y.F.); care1990@tju.edu.cn (Wei L.); 18202520278@163.com (Wen L.); 15002257297@163.com (M.G.); ihsan.chem@tju.edu.cn (I.U.)

[2] Tianjin University-Helmholtz-Zentrum Geesthacht, Joint Laboratory for Biomaterials and Regenerative Medicine, Tianjin 300072, China

[3] Key Laboratory of Systems Bioengineering of Ministry of Education, Tianjin University, Tianjin 300072, China

[4] Department of Physiology and Pathophysiology, Logistics University of Chinese People's Armed Police Force, Tianjin 300162, China

* Correspondence: renxiangkui@tju.edu.cn (X.R.); wenchen78084@163.com (W.Z.); Tel./Fax: +86-22-2740-1999 (X.R.)

Abstract: Biomimetic scaffolds have been investigated in vascular tissue engineering for many years. Excellent biodegradable materials are desired as temporary scaffolds to support cell growth and disappear gradually with the progress of guided tissue regeneration. In the present paper, a series of biodegradable copolymers were synthesized and used to prepared micro/nanofibrous scaffolds for vascular tissue engineering. Poly(lactide-*co*-glycolide-*co*-3(*S*)-methyl-morpholine-2,5-dione) [P(LA-*co*-GA-*co*-MMD)] copolymers with different L-lactide (LA), glycolide (GA), and 3(*S*)-methyl-2,5-morpholinedione (MMD) contents were synthesized using stannous octoate as a catalyst. Moreover, the P(LA-*co*-GA-*co*-MMD) nanofibrous scaffolds were prepared by electrospinning technology. The morphology of scaffolds was analyzed by scanning electron microscopy (SEM), and the results showed that the fibers are smooth, regular, and randomly oriented with diameters of 700 ± 100 nm. The weight loss of scaffolds increased significantly with the increasing content of MMD, indicating good biodegradable property of the scaffolds. In addition, the cytocompatibility of electrospun nanofibrous scaffolds was tested by human umbilical vein endothelial cells. It is demonstrated that the cells could attach and proliferate well on P(LA-*co*-GA-*co*-MMD) scaffolds and, consequently, form a cell monolayer fully covering on the scaffold surface. Furthermore, the P(LA-*co*-GA-*co*-MMD) scaffolds benefit to excellent cell infiltration after subcutaneous implantation. These results indicated that the P(LA-*co*-GA-*co*-MMD) nanofibrous scaffolds could be potential candidates for vascular tissue engineering.

Keywords: electrospinning; nanofibrous scaffolds; vascular tissue engineering; copolymers

1. Introduction

Cardiovascular diseases are one of the most frequent causes of death all over the world [1]. In the last three decades the demand for artificial blood vessels has increased due to a higher incidence of cardiovascular diseases [2]. Tissue engineering is emerging as a potential solution

for tissue and organ transplantations [3]. However, the small-diameter, synthetic vascular grafts are encountered in several problems such as thrombosis, intimal hyperplasia, and lower long-term patency rates in clinical application [1,4]. The ideal vascular tissue engineering scaffolds should be designed to mimic the native extracellular matrix (ECM) in order to regulate cellular behavior [5]. Native ECM is an interconnected 3D porous structure consisting of proteins and carbohydrate biopolymers, which provides suitable environment for cells to adhere, grow, and proliferate [6]. Native ECM structure can be mimicked through many ways, such as drawing [7], template synthesis [8], temperature-induced phase separation [9], molecular self-assembly [10], and electrospinning [11–15]. Among these strategies, electrospinning technology is regarded as an efficient preparation method because it can produce nanofibrous scaffolds with interconnected pores, high porosity, and large surface area to mimic native ECM [16–22].

In addition, materials also play an important role in most vascular tissue engineering strategies. The ideal materials for vascular tissue engineering should have excellent biocompatibility, good mechanical properties, and appropriate degradation behavior [23]. Biodegradable polymers, such as poly(L-lactic acid) (PLLA), poly(glycolic acid) (PGA) and poly(lactic-*co*-glycolic acid) (PLGA), have drawn a lot of attention in research because of their well-characterized biodegradable properties [24–28]. These materials have been successfully used in bone tissue, vessel, and patches for wounds [29–31]. Among these biodegradable polymers, PLGA is one of the most widely used classes of polymers for vascular tissue engineering, which has been already approved by the Food and Drug Administration (FDA) as a constituent of many biomaterial-based devices [28].

Currently, polydepsipeptides have been widely accepted as a valuable class of synthetic biodegradable polymers because the strong intermolecular hydrogen-bond interaction between the amide groups can achieve a higher reactivity in ring-opening polymerization (ROP), and the presence of easily hydrolysable ester linkages and amide-bonds can ensure high degradability [32–35]. In 1985, Helder *et al.* synthesized polydepsipeptides by ROP of morpholine-2,5-dione derivatives for the first time [36]. Since then, morpholine-2,5-dione derivatives, which have an ester group and an amide group in one six-membered ring, have been used to synthesize various biodegradable copolymers [37–39].

In particular, 3(*S*)-methyl-morpholine-2,5-dione (MMD), which possesses a better performance of polymerization than other morpholine-2,5-dione derivatives with large substitutes, has been a promising derivative to develop biodegradable drug delivery systems [35]. Meanwhile, the copolymers synthesized from MMD shows different crystallization degrees owing to the optical activity of the monomer [35,40,41]. Moreover, the degradation products of MMD including L-amino acids can stimulate the proliferation of endothelial cells via a signal pathway and be properly metabolized by living tissues [42–45]. Based on the copolymers of MMD with other cyclic monomers, our group have developed some gene delivery systems for promoting the transfection and migration of endothelial cells [42,46–49]. However, to the best of our knowledge, the study on electrospun nanofibrous scaffolds from the copolymers of MMD with other cyclic monomers for vascular tissue engineering has not been reported previously.

In this article, poly(lactide-*co*-glycolide-*co*-3(*S*)-methyl-morpholine-2,5-dione) P(LA-*co*-GA-*co*-MMD) copolymers were synthesized by ROP of L-lactide (LA), glycolide (GA) and MMD using stannous octoate (Sn(Oct)$_2$) as a catalyst. Their structural characteristics and molecular weights were identified or determined by ^{1}H NMR, FT-IR, and gel permeation chromatography (GPC) analysis. Moreover, electrospinning was employed to prepare the P(LA-*co*-GA-*co*-MMD) nanofibrous scaffolds for potential use in vascular tissue engineering. The mechanical properties of electrospun P(LA-*co*-GA-*co*-MMD) scaffolds were investigated under dry and wet conditions. The degradation behavior of the scaffolds were investigated in phosphate buffered saline (PBS) solution at 37 °C for 28 days. The proliferation of human umbilical vein endothelial cells (HUVECs) on scaffolds were studied by SEM and thiazolyl blue assay (MTT). The cell infiltration of P(LA-*co*-GA-*co*-MMD) scaffolds were investigated by subcutaneous implantation.

2. Experimental Section

2.1. Materials

Sn(Oct)$_2$ was purchased from Sigma-Aldrich (Beijing, China). GA and LA were obtained from Foryou Medical Device Co., Ltd. (Huizhou, China). MMD monomer was prepared using our previously reported method [50]. All the other chemicals were purchased from Tianjin Jiangtian Chemical Technology Co., Tianjin, Ltd, China. These chemicals were of analytical grade and used without further purification.

2.2. Synthesis of Copolymer PLGA and P(LA-co-GA-co-MMD)

2.2.1. Synthesis of Copolymer PLGA

PLGA (LA/GA = 75/25, *w*/*w*) was synthesized by ROP of LA and GA using Sn(Oct)$_2$ as a catalyst.

2.2.2. Synthesis of P(LA-*co*-GA-*co*-MMD) Copolymers

LA, GA, MMD and Sn(Oct)$_2$ toluene solution were added into a Schlenk and submitted to vacuum/nitrogen cycles. The Schlenk was finally sealed under dry nitrogen and was immersed into an oil bath previously heated to 120 °C for 24 h. The copolymer was dissolved in chloroform and precipitated in *n*-hexane, repeated this process for three times, and dried at room temperature for 24 h under vacuum. Finally, the copolymers named as P(LA-*co*-GA-*co*-MMD)$_1$, P(LA-*co*-GA-*co*-MMD)$_2$ and P(LA-*co*-GA-*co*-MMD)$_3$ were obtained, where the subscript 1, 2, and 3 stand for different LA/GA/MMD contents in copolymers as described in Table 1.

Table 1. The synthesis yields, molecular weights, and contents of LA, GA, and MMD in copolymers.

Sample ID	Weight Content [a]/%			Yield wt %	M_n [b]/10^4	M_w [b]/10^4	PDI [b]
	LA	GA	MMD				
PLGA	70.1	29.9	0	80.3	5.19	11.89	2.29
P(LA-*co*-GA-*co*-MMD)$_1$	70.3	24.2	5.5	82.1	5.74	13.35	2.33
P(LA-*co*-GA-*co*-MMD)$_2$	66.1	20.9	13.0	78.4	4.67	10.88	2.33
P(LA-*co*-GA-*co*-MMD)$_3$	60.9	21.7	17.4	76.8	4.08	9.44	2.32

[a] Estimated by ^{1}H NMR; [b] Determined by GPC; PLGA, poly(lactic-*co*-glycolic acid); LA, L-lactide; GA, glycolide; MMD, 3(*S*)-methyl-2,5-morpholinedione; PDI, polydispersity index.

2.3. Preparation of Spinning Solution

PLGA, P(LA-*co*-GA-*co*-MMD)$_1$, P(LA-*co*-GA-*co*-MMD)$_2$, and P(LA-*co*-GA-*co*-MMD)$_3$ were dissolved in chloroform (CHCl$_3$) and *N*,*N*-dimethylformamide (DMF) solvent in 7:3 volume ratio to prepare 20 *w*/*v* % spinning solution separately.

2.4. Fabrication of the Electrospun Scaffolds

The spinning solution was fed into a syringe with a blunt metal needle tip. The needle tip with the inner diameter of 0.5 mm was clamped by a high voltage power supply (Model, 0–50 kV, Tianjin Dongwen high voltage power supply company, Tianjin, China). The spinning solution was delivered by a syringe pump (749000-05, Cole-Parmer instrument company, Beijing, China) and the applied voltage, feed rate, target distance, temperature, and rotating speed of the collector were 18 kV, 0.6 mL/h, 15 cm, 25 °C, and 200 r/min, respectively. The electrospun fibers were collected on a metal plate covered with aluminum foil and placed into a vacuum oven at room temperature to evaporate residue solvents.

2.5. Characterization

FT-IR spectra of the copolymers were obtained using a FT-IR spectrometer (FTS-6000, Bio-Rad, Hercules, CA, USA). ^{1}H NMR spectra of the synthesized copolymers were recorded with a Bruker Avance spectrometer (AV-400, Bruker, Karlsruhe, Gemany) operating at 400 MHz in DMSO-d$_6$.

The surface morphology of scaffolds was analyzed by field emission scanning electron microscope (S-4800, Hitachi, Tokyo, Japan) at an accelerating voltage of 10 kV, after sputter coating with gold. The fiber average diameters were calculated by measuring not less than 50 randomly selected fibers from SEM micrographs using Digimizer software (Tianyan Rongzhi, Beijing, China).

The mechanical properties of electrospun nanofibrous scaffolds were determined using a tensile testing instrument (WDW-02, Changchun, China) equipped with a 100 N load cell at a cross-head speed of 5 mm/min. The nanofibrous scaffolds were cut into rectangle with length of 20 mm, width of 5 mm and thickness measured with thickness meter, and then tested in dry and wet conditions (immersion in PBS solution for 1 h at room temperature to simulate the application condition). Five samples of each electrospun scaffold were tested to calculate an average value.

The PLGA and P(LA-*co*-GA-*co*-MMD) nanofibrous scaffolds were cut into rectangles with lengths of 20 mm, widths of 10 mm, and weighed accurately, then put them into 10 mL PBS solution (pH = 7.4) at 37 °C to test their degradation behavior. At different time intervals, the scaffolds were removed from PBS solution and washed three times with distilled water and placed in a vacuum oven for 24 h. After weighing accurately, the weight loss was calculated according to the following equation:

$$\text{Weight loss} \, (\%) \; = \; (W_0 - W_i)/W_0 \times 100\% \tag{1}$$

where W_i is the mass of the scaffolds after degradation for i days, and W_0 is the mass of the scaffolds before degradation.

2.6. In Vitro Cell Culture Experiment

Human umbilical vein endothelial cells (HUVECs) (Tianjin Hospital of Armed Police Forces, Tianjin, China) were cultured in Dulbecco's modified Eagle medium (DMEM, Gibco, Waltham, MA, USA) with supplements of 10% fetal bovine serum (FBS, Gibco), 100 μg/mL penicillin, and 100 μg/mL streptomycin, in a humidified atmosphere of 5% CO_2 at 37 °C. The adherent cells were cultured to confluence, and the medium was exchanged every two days.

2.7. Cell Seeding and Morphology Observation

Nanofibrous scaffolds were cut to fit the size of 96-well plate and sterilized by being soaked in 75% ethanol for 30 min, then washed thoroughly by PBS solution (pH = 7.4). Then the scaffolds were put into 96-well culture plates. HUVECs were trypsinized, counted, and then plated at a density of 1×10^4 cells/well onto the surface of scaffolds. In order to avoid scaffold floating, thin glass rings fitting the inner diameter of the wells were used. Cellularized scaffolds were incubated at 37 °C in 5% CO_2.

After 7 days of cell culture, the nanofibrous scaffolds were harvested, and washed with PBS to remove non-adherent cells and then fixed in 2.5% glutaraldehyde for 2 h at room temperature. The scaffolds were dehydrated using series of graded alcohol solutions from 50% to 100% in steps of 10% for 10 min, and then lyophilized. To evaluate cell morphology and adhesion to the scaffolds, SEM was employed at an accelerating voltage of 10 kV.

2.8. MTT Assay

Thiazolyl blue assay was performed at time point of one, three, and secen days to determine the relative cell viability in each well. Scaffolds were sterilized and pre-wetted as above described. HUVECs were seeded at a density of 1×10^4 cells/well onto the scaffolds in 96-well culture plate. Briefly, 20 μL of MTT (5 mg/mL) was added to each well and incubated at 37 °C in 5% CO_2 for 4 h in

humidified atmosphere. At the end of assay, the purple formazan reaction product was dissolved by adding 150 μL dimethyl sulfoxide (DMSO) and vibrated slightly for 10 min, and then 100 μL solution was transferred into a new 96-well plate. The absorbance of each sample was measured using an ELISA reader at 490 nm. The relative cell viability (%) was calculated according to the following equation:

$$\text{Relative cell viability} = \text{OD490}'/\text{avg}(\text{OD490}') \times 100\% \tag{2}$$

where OD490$'$ is the absorbance value of experimental well minus zero wells and avg(OD490$'$) is the average absorbance value of control wells minus zero wells.

2.9. Subcutaneous Implantation

Sixteen Sprague-Dawley rats (male, 150–200 g) were used for this study. The investigation conforms to the Guide for the Care and Use of Laboratory Animals published by the US National Institutes of Health (NIH Publication 8th Edition, 2011). The animal experimental protocol was approved by the Animal Care and Use Ethics Committee of the Logistics University of Chinese People's Armed Police Force. The scaffolds were treated with a 70% ethanol solution overnight and then stored in sterile filtered PBS solution before implantation. These rats were randomly assigned to four groups (two specimens in each rat) to implant PLGA, P(LA-*co*-GA-*co*-MMD)$_1$, P(LA-*co*-GA-*co*-MMD)$_2$, and P(LA-*co*-GA-*co*-MMD)$_3$ scaffolds. After seven days, the scaffolds were explanted and fixed in 10% buffered formalin solution for two days. Once the dehydration procedure was completed, each specimen was embedded in paraffin and sectioned into 5 μm slice. The sections were stained with hematoxylin and eosin (H and E) for histological analyses.

3. Results and Discussion

3.1. Synthesis of P(LA-co-GA-co-MMD) Copolymers

The synthesis of P(LA-*co*-GA-*co*-MMD) copolymers is shown in Scheme 1. The PLGA and P(LA-*co*-GA-*co*-MMD) copolymers were synthesized by ROP of LA, GA,s and MMD using Sn(Oct)$_2$ as catalyst. As shown in Table 1, the contents of LA, GA and MMD in copolymers and the molecular weights of copolymers were estimated by ^{1}H NMR and GPC, respectively. The yields of the copolymerization were in the range of 75%–85%. The MMD contents in P(LA-*co*-GA-*co*-MMD)$_1$, P(LA-*co*-GA-*co*-MMD)$_2$ and P(LA-*co*-GA-*co*-MMD)$_3$ copolymers were estimated to be 5.5%, 13.0% and 17.4%, respectively. And the number-averaged molecular weights and polydispersity indexes of copolymers were in the range of 4.08×10^4–5.74×10^4 and 2.29–2.33, respectively.
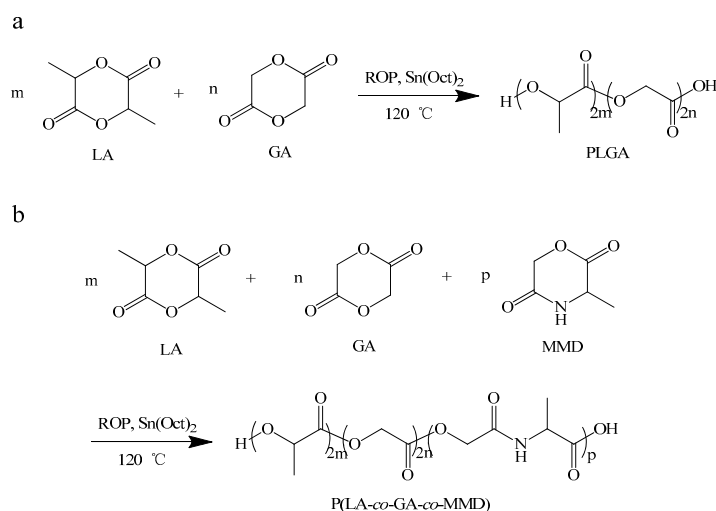
Scheme 1. Synthesis of PLGA copolymers (**a**) and P(LA-*co*-GA-*co*-MMD) copolymers (**b**).

As shown in Figure 1, FT-IR spectra of P(LA-*co*-GA-*co*-MMD) copolymers presented a strong signal at 1753 cm^{-1} which indicated the carbonyl group (–C=O) in the copolymers. The stretching frequency at 1091 cm^{-1} indicated the ester group (–O–C=O), and the absorption bands at 1683 cm^{-1} as well as the broad absorption band from 3200 to 3400 cm^{-1} assigned to the stretching of secondary amide (–NH–) group. It was found that the characteristic peaks of the secondary amide (–NH–) was obviously displayed in the copolymers and the relative adsorption intensity of these peaks became stronger along with the increasing MMD content in P(LA-*co*-GA-*co*-MMD) copolymers. These results suggested that P(LA-*co*-GA-*co*-MMD) copolymers were synthetized successfully.
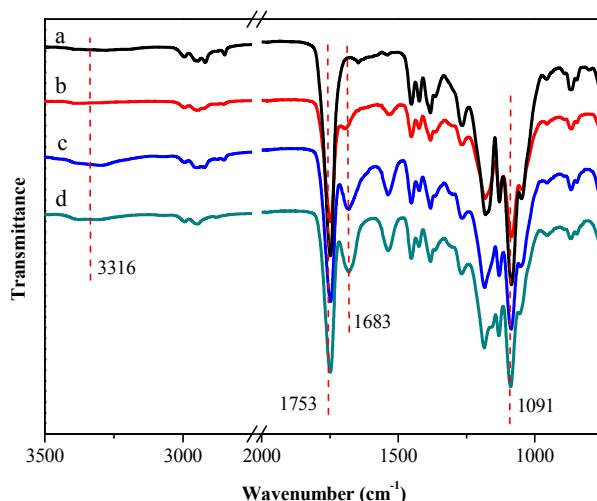

Figure 1. FT-IR spectra of PLGA and P(LA-*co*-GA-*co*-MMD) copolymers. (**a**) PLGA; (**b**) P(LA-*co*-GA-*co*-MMD)$_1$; (**c**) P(LA-*co*-GA-*co*-MMD)$_2$; and (**d**) P(LA-*co*-GA-*co*-MMD)$_3$.

The ^{1}H NMR spectra of PLGA and P(LA-*co*-GA-*co*-MMD)$_3$ copolymers are shown in Figure 2. The presence of methine (–CH) and methyl (–CH$_3$) protons in LA was observed at around 5.21 ppm (c) and 1.50 ppm (a), respectively. The evidence for methane (–CH$_2$) in GA occurred at around 4.85 ppm (b). As shown in Figure 2b, the methine (–CH), methane (–CH$_2$) and methyl (–CH$_3$) protons in MMD were observed at around 4.40 ppm (e), 4.60 ppm (g) and 1.35 ppm (f), respectively. The evidence for secondary amide (–NH–) in MMD occurred at around 8.53 ppm (d). These results suggested that P(LA-*co*-GA-*co*-MMD) copolymers were synthetized successfully.
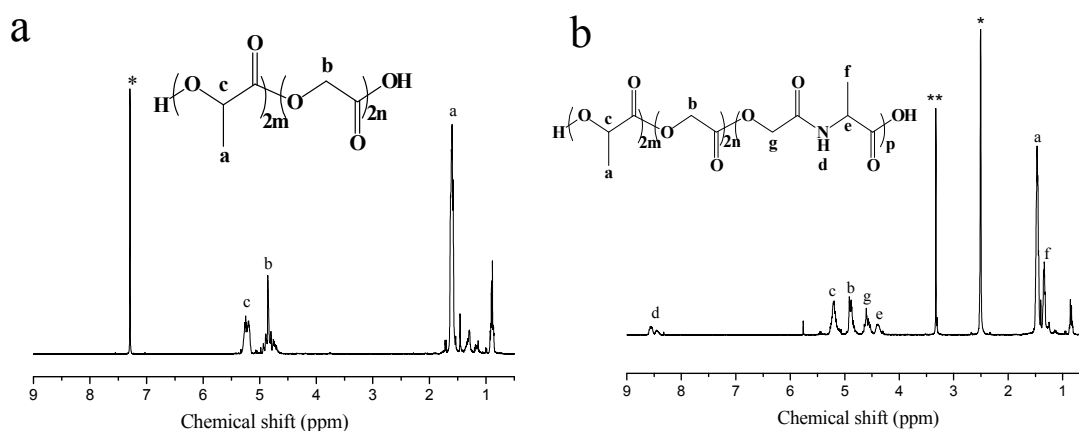

Figure 2. ^{1}H NMR spectra of PLGA and P(LA-*co*-GA-*co*-MMD)$_3$ copolymers. (**a**) ^{1}H NMR spectra of PLGA copolymer in CDCl$_3$; (**b**) ^{1}H NMR spectra of P(LA-*co*-GA-*co*-MMD) copolymer in DMSO-d$_6$, * Solvent peak; ** H$_2$O peaks.

3.2. Morphology of PLGA and P(LA-co-GA-co-MMD) Scaffolds

The morphology of the scaffolds plays an important role in vascular tissue engineering. The scaffold fibers should be uniform and smooth. The beaded and non-uniform scaffolds could be avoided by optimizing solvent system, concentration of the spinning solution, applied voltage, flow rate, temperature, target distance, and rotating speed of collector [51]. The morphology of electrospun PLGA and P(LA-*co*-GA-*co*-MMD) scaffolds was characterized by SEM and shown in Figure 3. It revealed that the fibers are randomly oriented and appear to be uniform and smooth. Quantitative analysis indicated fiber diameters of 650 ± 150, 750 ± 120, 670 ± 130, and 700 ± 100 nm for electrospun PLGA, P(LA-*co*-GA-*co*-MMD)$_1$, P(LA-*co*-GA-*co*-MMD)$_2$, and P(LA-*co*-GA-*co*-MMD)$_3$ scaffolds, respectively. There was no significant difference in the fiber diameters among PLGA and those P(LA-*co*-GA-*co*-MMD) scaffolds with different contents of MMD. It might be attributed to the same electrospuning conditions of PLGA and P(LA-*co*-GA-*co*-MMD) scaffolds.
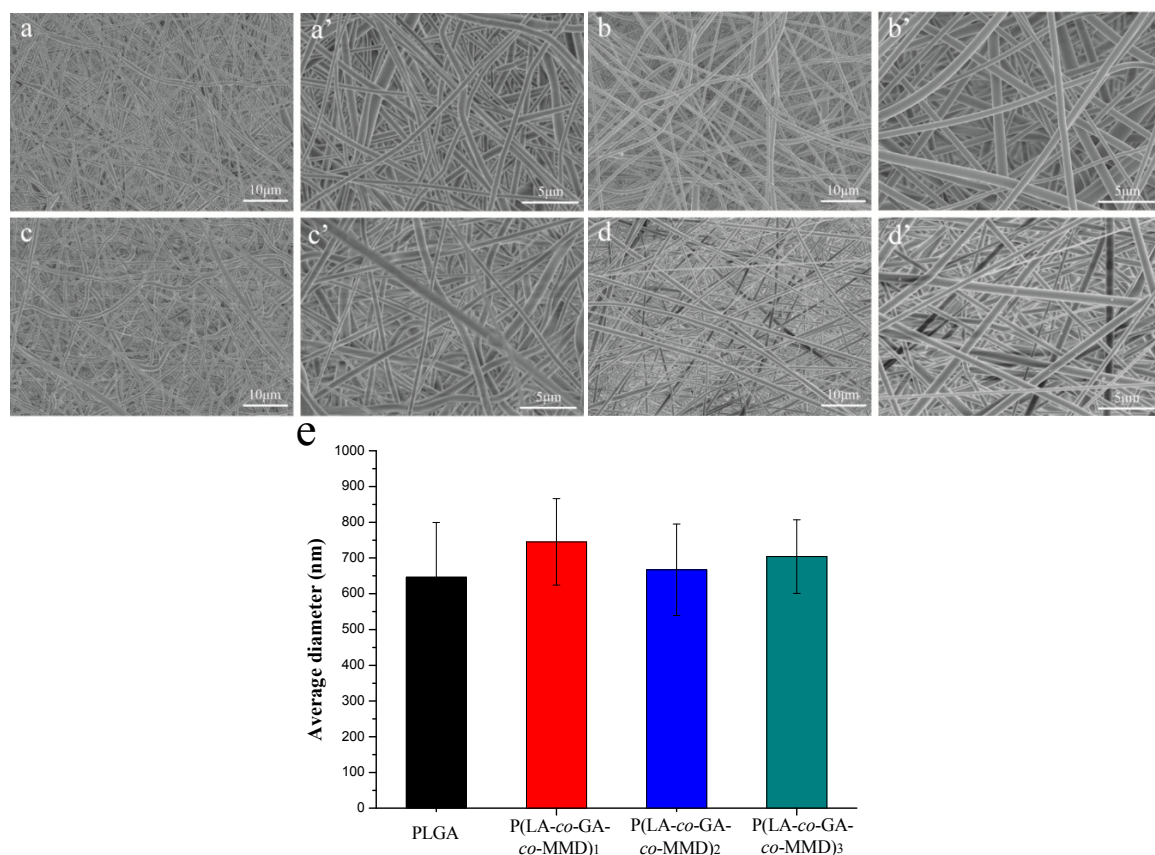

Figure 3. SEM of electrospun nanofibrous scaffolds: (**a** and **a'**) PLGA; (**b** and **b'**) P(LA-*co*-GA-*co*-MMD)$_1$; (**c** and **c'**) P(LA-*co*-GA-*co*-MMD)$_2$; (**d** and **d'**) P(LA-*co*-GA-*co*-MMD)$_3$ and (**e**) average diameters of electrospun scaffolds. (mean $\pm$ SD, $n = 3$).

3.3. Mechanical Properties of PLGA and P(LA-co-GA-co-MMD) Scaffolds

The mechanical properties of vascular tissue engineering scaffolds are quite important to evaluate whether they are recommended for biomedical application. The mechanical properties of PLGA and P(LA-*co*-GA-*co*-MMD) nanofibrous scaffolds in dry and wet conditions were summarized in Table 2. It's well known that the tensile strength of natural coronary artery is about 1.4–11.14 MPa, and elongation at break is usually above 40% [52]. Previous studies showed that the tensile strength and elongation at break of PLGA-based nanofibrous scaffolds were about 2–6 MPa and 80%–140% [5,53–56]. Here, the tensile strength and elongation at break of PLGA and P(LA-*co*-GA-*co*-MMD) nanofibrous

scaffolds at dry condition were in the range of 2.63–3.23 MPa and 84%–117%, respectively, which could meet the mechanical requirement for transplantation of vascular scaffolds. There were no significant differences of mechanical properties between electrospun PLGA and P(LA-*co*-GA-*co*-MMD) nanofibrous scaffolds in dry condition. Under the wet condition, the tensile strength and elongation at break of PLGA and P(LA-*co*-GA-*co*-MMD) nanofibrous scaffolds were also in the range of 1.89–2.46 MPa and 114%–559%, respectively. The tensile strength slightly reduced compared with the dry condition for the same nanofibrous scaffold. And the elongation at break of the same nanofibrous scaffold in wet condition was much higher than that in dry condition. Moreover, the elongations at break of scaffolds under wet condition increased significantly with the increasing contents of MMD in copolymers. For P(LA-*co*-GA-*co*-MMD)$_3$ nanofibrous scaffold, the elongation at break was 559% $\pm$ 82%, significantly higher than the other PLGA-based scaffolds.

Table 2. Mechanical properties of PLGA and P(LA-*co*-GA-*co*-MMD) scaffolds under dry and wet conditions.

Sample ID	Tensile Strength (MPa)		Elongation at Break (%)	
	Dry	Wet	Dry	Wet
PLGA	2.89 $\pm$ 0.31	2.20 $\pm$ 0.12	84 $\pm$ 5	114 $\pm$ 20
P(LA-*co*-GA-*co*-MMD)$_1$	2.63 $\pm$ 0.20	2.46 $\pm$ 0.27	105 $\pm$ 28	242 $\pm$ 34
P(LA-*co*-GA-*co*-MMD)$_2$	2.66 $\pm$ 0.07	1.89 $\pm$ 0.46	109 $\pm$ 25	363 $\pm$ 32
P(LA-*co*-GA-*co*-MMD)$_3$	3.23 $\pm$ 0.61	2.20 $\pm$ 0.68	117 $\pm$ 9	559 $\pm$ 82

3.4. In Vitro Degradation of PLGA and P(LA-co-GA-co-MMD) Scaffolds

Degradation behavior influences directly on the application of the scaffolds. The ideal materials for tissue engineering are desired as temporary scaffolds to support cell growth and disappear with the progress of tissue regeneration. The degradation behavior of electrospun PLGA and P(LA-*co*-GA-*co*-MMD) nanofibrous scaffolds in PBS solution (pH = 7.4) at 37 °C for 28 days was investigated based on their weight loss. As shown in Figure 4, after 14 days of degradation, there was a little weight reduction for all scaffolds. The weight loss was 8.2% $\pm$ 1.0%, 10.2% $\pm$ 1.6%, 12.3% $\pm$ 1.2%, and 14.9% $\pm$ 1.5% for PLGA, P(LA-*co*-GA-*co*-MMD)$_1$, P(LA-c*o*-GA-*co*-MMD)$_2$, and P(LA-*co*-GA-*co*-MMD)$_3$ scaffolds, respectively. Then, the weights of all scaffolds were continuously decreased and the P(LA-*co*-GA-*co*-MMD)$_3$ nanofibrous scaffold showed the largest weight loss. At 28 days, the weight loss of PLGA, P(LA-*co*-GA-*co*-MMD)$_1$, P(LA-c*o*-GA-*co*-MMD)$_2$, and P(LA-*co*-GA-*co*-MMD)$_3$ were 16.7% $\pm$ 2.5%, 25.9% $\pm$ 3.4%, 41.2% $\pm$ 5.3%, and 52.8% $\pm$ 6.8%. Generally, the weight loss of PLGA scaffold was lower than that of P(LA-*co*-GA-*co*-MMD) scaffolds. The degradation behavior was found to depend strongly on the MMD contents in the copolymers and the weight loss of electrospun P(LA-*co*-GA-*co*-MMD) nanofibrous scaffolds increased with the increasing content of MMD in copolymers. It was mainly attributed to the faster hydrolysis of MMD residue, and the MMD residue contains both ester and amide groups in the main chain which ensure high degradability [35,37]. These results suggested that the P(LA-*co*-GA-*co*-MMD) nanofibrous scaffolds had good biodegradable property and the degradability of scaffolds could be controlled by varying the contents of MMD in the copolymers.

3.5. Proliferation of HUVECs on PLGA and P(LA-co-GA-co-MMD) Scaffolds

The proliferation behavior of HUVECs on PLGA and P(LA-*co*-GA-*co*-MMD) nanofibrous scaffolds was determined by MTT assay for one, three, and seven days and the results were shown in Figure 5. The relative cell viability was increasing over time for the same scaffold. At the first day, the relative cell viability of PLGA, P(LA-*co*-GA-*co*-MMD)$_1$, P(LA-c*o*-GA-*co*-MMD)$_2$, and P(LA-*co*-GA-*co*-MMD)$_3$ was 69.0% $\pm$ 5.7%, 56.2% $\pm$ 5.8%, 49.8% $\pm$ 4.1% and 45.8% $\pm$ 3.2%, respectively. It demonstrated that the electrospun scaffolds were highly biocompatible and non-cytotoxic, and illustrated that the scaffolds

were favorable for cell attachment. However, the relative cell viability on the P(LA-*co*-GA-*co*-MMD) scaffolds was lower than that of PLGA scaffold at the first day. After culturing for seven days, the relative cell viability were 91.2% ± 5.4%, 95.1% ± 3.2%, 95.9% ± 11.2%, and 103.1% ± 9.1% for PLGA, P(LA-*co*-GA-*co*-MMD)$_1$, P(LA-c*o*-GA-*co*-MMD)$_2$, and P(LA-*co*-GA-*co*-MMD)$_3$ nanofibrous scaffolds, respectively. The relative cell viability of HUVECs on P(LA-*co*-GA-*co*-MMD) nanofibrous scaffolds increased with the increasing contents of MMD in copolymers and HUVECs on the P(LA-*co*-GA-*co*-MMD)$_3$ scaffolds exhibited the highest relative cell viability. The main reason was the degradation product (L-alanine) of MMD in P(LA-*co*-GA-*co*-MMD) copolymers might promote the proliferation of HUVECs via a signal pathway [43]. These results were in good agreement with our previous studies [42,46].
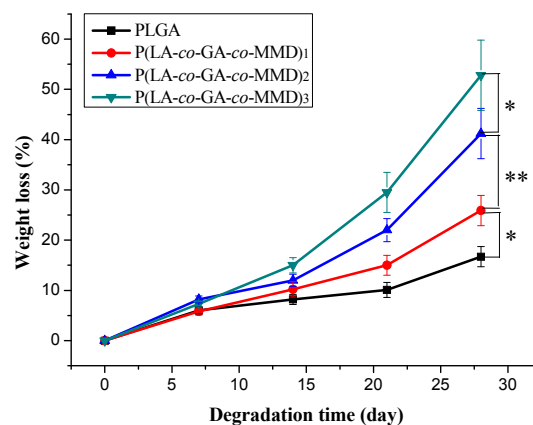

Figure 4. *In vitro* degradation of PLGA and P(LA-*co*-GA-*co*-MMD) nanofibrous scaffolds in PBS solution (pH = 7.4) at 37 °C for 28 days. (mean ± SD, *n* = 3, * *p* ⩽ 0.05, ** *p* ⩽ 0.01).
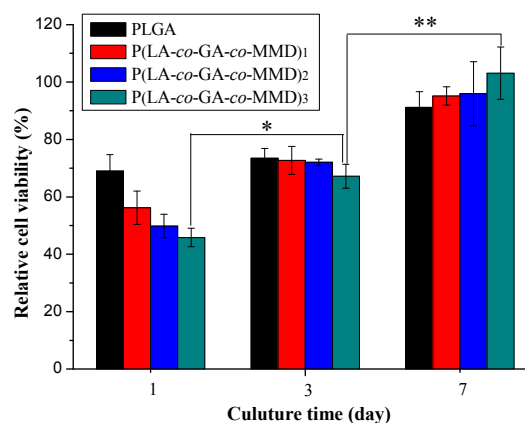

Figure 5. The relative cell viability of HUVECs cultured on PLGA and P(LA-*co*-GA-*co*-MMD) nanofibrous scaffolds. (mean ± SD, *n* = 3, * *p* ⩽ 0.05, ** *p* ⩽ 0.01).

To investigate the cell adhesion and proliferation, HUVECs were cultured on electrospun PLGA and P(LA-*co*-GA-*co*-MMD) scaffolds. After culturing for seven days, the cell adhesion behavior was observed by SEM, and the images were presented in Figure 6. It was observed that the HUVECs could adhere and grow well on the surface of all scaffolds; the cells could closely adhere on the fibrous surface and stretch across the randomly interconnected structures. However, considering the areas covered with cells on the scaffolds, the cell numbers of attachment and growth on the P(LA-*co*-GA-*co*-MMD) scaffolds were higher than those of PLGA scaffold, which was consistent with the MTT assay. These results demonstrated that the P(LA-*co*-GA-*co*-MMD) scaffolds could promote the cell adhesion and proliferation.
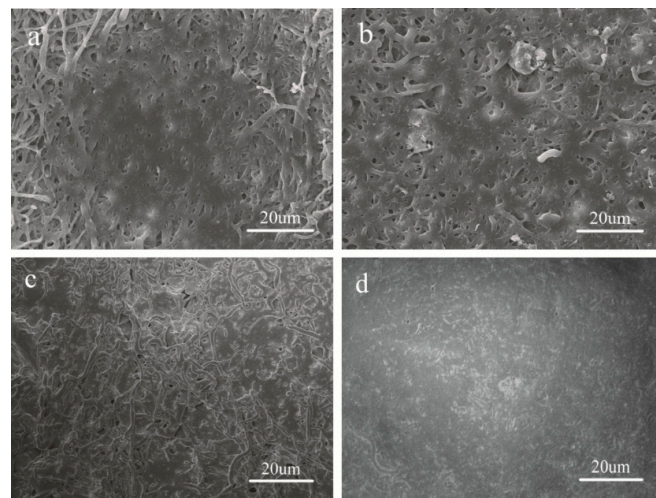
Figure 6. SEM of HUVECs cultured on electrospun nanofibrous scaffolds: (**a**) PLGA; (**b**) P(LA-*co*-GA-*co*-MMD)$_1$; (**c**) P(LA-*co*-GA-*co*-MMD)$_2$; and (**d**) P(LA-*co*-GA-*co*-MMD)$_3$.

3.6. Tissue Response of Scaffold in Subcutaneous Implantation

The vascular scaffolds should possess excellent biocompatibility. Biocompatibility indicates the ability of a material to perform with an appropriate tissue response. The tissue responses of scaffolds were evaluated via subcutaneous implantation in Sprague-Dawley rats. Histological analysis was carried out after seven day-implantation in order to evaluate cell infiltration and the representative images were shown in Figure 7. In general, all the explanted scaffolds showed the cell infiltration. For PLGA scaffold, the cell attachment and infiltration mainly occurred on the surface of the scaffold and only a few cells could infiltrate deeply into the internal structure. The case of P(LA-*co*-GA-*co*-MMD) scaffolds was completely different, where most of the cells had infiltrated deeply into the internal structure. The possible reason was that P(LA-*co*-GA-*co*-MMD) scaffolds could undergo relatively fast degradation after subcutaneous implantation. As a result, some fibers were broken and the pore size of the scaffolds became large, which was favorable for the cells easily to infiltrate deeply into the internal structure.
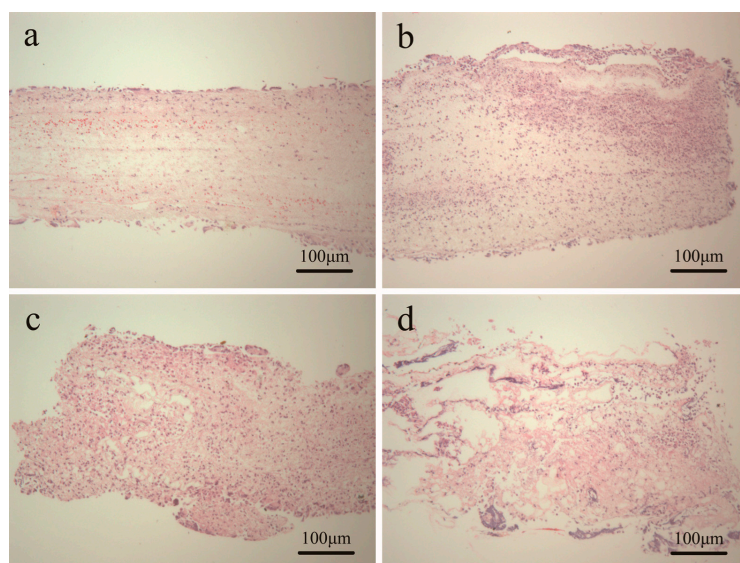

Figure 7. H and E images of subcutaneous implanted scaffolds for seven days: (**a**) PLGA; (**b**) P(LA-*co*-GA-*co*-MMD)$_1$; (**c**) P(LA-*co*-GA-*co*-MMD)$_2$; and (**d**) P(LA-*co*-GA-*co*-MMD)$_3$.

In order to overcome the thrombogenicity and compliance mismatch in small diameter vessel reconstruction, researchers have focused on tissue engineering and biodegradable scaffolds to develop "living" vascular grafts. The ideal vascular scaffolds should provide the initial strength, and then gradually degrade and cells grow to create a graft composed solely of host tissue. We have developed a series of biodegradable scaffolds based on P(LA-*co*-GA-*co*-MMD) copolymers. It showed excellent degradation behavior compared with PLGA scaffold, and the degradability of the P(LA-*co*-GA-*co*-MMD) scaffolds could be controlled by varying the contents of MMD in the copolymers. Furthermore, the scaffolds could provide a suitable environment for ECs to adhere, grow and proliferate.

4. Conclusions

In this study, P(LA-*co*-GA-*co*-MMD) copolymers were synthesized by ROP of LA, GA, and MMD using Sn(Oct)$_2$ as catalyst. Then, biodegradable P(LA-*co*-GA-*co*-MMD) scaffolds were prepared by electrospinning technology. The P(LA-*co*-GA-*co*-MMD) scaffolds showed good mechanical properties and the weight loss is higher than PLGA scaffolds, which indicates the good biodegradable property of the scaffold. In addition, the HUVECs could attach and proliferate well on the P(LA-*co*-GA-*co*-MMD) scaffolds to form a cell monolayer fully covering on scaffold surface. Furthermore, cells could infiltrate well into the P(LA-*co*-GA-*co*-MMD) scaffolds after subcutaneous implantation. These results indicated that the P(LA-*co*-GA-*co*-MMD) nanofibrous scaffolds could be potential candidates for vascular tissue engineering.

Author Contributions: Wei Lu performed experiments and wrote the manuscript. Wen Liu performed cell culture and MTT assay. Mengyang Guo, Ihsan Ullah and Xiangkui Ren were involved in data analysis. Yakai Feng, Wencheng Zhang and Xiangkui Ren directed the research. All authors proof-read and approved the manuscript.

Conflicts of Interest: The authors declare no conflict of interest.

References

1. Wang, H.; Feng, Y.; Zhao, H.; Xiao, R.; Lu, J.; Zhang, L.; Guo, J. Electrospun hemocompatible PU/gelatin-heparin nanofibrous bilayer scaffolds as potential artificial blood vessels. *Macromol. Res.* **2012**, *20*, 347–350. [CrossRef]
2. Lovett, M.; Cannizzaro, C.; Daheron, L.; Messmer, B.; Vunjak-Novakovic, G.; Kaplan, D.L. Silk fibroin microtubes for blood vessel engineering. *Biomaterials* **2007**, *28*, 5271–5279. [CrossRef] [PubMed]
3. Dong, Y.; Liao, S.; Ngiam, M.; Chan, C.K.; Ramakrishna, S. Degradation behaviors of electrospun resorbable polyester nanofibers. *Tissue Eng. B Rev.* **2009**, *15*, 333–351. [CrossRef] [PubMed]
4. Kidoaki, S.; Kwon, I.K.; Matsuda, T. Mesoscopic spatial designs of nano-and microfiber meshes for tissue-engineering matrix and scaffold based on newly devised multilayering and mixing electrospinning techniques. *Biomaterials* **2005**, *26*, 37–46. [CrossRef] [PubMed]
5. Zhou, W.; Feng, Y.; Yang, J.; Fan, J.; Lv, J.; Zhang, L.; Guo, J.; Ren, X.; Zhang, W. Electrospun scaffolds of silk fibroin and poly(lactide-*co*-glycolide) for endothelial cell growth. *J. Mater. Sci. Mater. Med.* **2015**, *26*, 5386. [CrossRef] [PubMed]
6. Yu, L.; Feng, Y.; Li, Q.; Hao, X.; Liu, W.; Zhou, W.; Shi, C.; Ren, X.; Zhang, W. PLGA/SF blend scaffolds modified with plasmid complexes for enhancing proliferation of endothelial cells. *React. Funct. Polym.* **2015**, *91–92*, 19–27. [CrossRef]
7. Nain, A.S.; Wong, J.C.; Amon, C.; Sitti, M. Drawing suspended polymer micro-/nanofibers using glass micropipettes. *Appl. Phys. Lett.* **2006**, *89*, 183105. [CrossRef]
8. Tao, S.L.; Desai, T.A. Aligned arrays of biodegradable poly(epsilon-caprolactone) nanowires and nanofibers by template synthesis. *Nano Lett.* **2007**, *7*, 1463–1468. [CrossRef] [PubMed]

9. Liu, X.; Smith, L.; Wei, G.; Won, Y.; Ma, P.X. Surface engineering of nano-fibrous poly (ʟ-lactic acid) scaffolds via self-assembly technique for bone tissue engineering. *J. Biomed. Nanotechnol.* **2005**, *1*, 54–60. [CrossRef]

10. Paramonov, S.E.; Jun, H.W.; Hartgerink, J.D. Self-assembly of peptide-amphiphile nanofibers: The roles of hydrogen bonding and amphiphilic packing. *J. Am. Chem. Soc.* **2006**, *128*, 7291–7298. [CrossRef] [PubMed]

11. Hohman, M.M.; Shin, M.; Rutledge, G.; Brenner, M.P. Electrospinning and electrically forced jets. I. Stability theory. *Phys. Fluids* **2001**, *13*, 2201–2220. [CrossRef]

12. Hohman, M.M.; Shin, M.; Rutledge, G.; Brenner, M.P. Electrospinning and electrically forced jets. II. Applications. *Phys. Fluids* **2001**, *13*, 2221–2236. [CrossRef]

13. Reneker, D.H.; Yarin, A.L.; Fong, H.; Koombhongse, S. Bending instability of electrically charged liquid jets of polymer solutions in electrospinning. *J. Appl. Phys.* **2000**, *87*, 4531–4547. [CrossRef]

14. Yarin, A.L.; Koombhongse, S.; Reneker, D.H. Taylor cone and jetting from liquid droplets in electrospinning of nanofibers. *J. Appl. Phys.* **2001**, *90*, 4836. [CrossRef]

15. Yarin, A.L.; Koombhongse, S.; Reneker, D.H. Bending instability in electrospinning of nanofibers. *J. Appl. Phys.* **2001**, *89*, 3018. [CrossRef]

16. Khan, M.; Yang, J.; Shi, C.; Feng, Y.; Zhang, W.; Gibney, K.; Tew, G.N. Surface modification of polycarbonate urethane with zwitterionic polynorbornene via thiol-ene click-reactionto facilitate cell growth and proliferation. *Macromol. Mater. Eng.* **2015**, *300*, 802–809. [CrossRef]

17. Khan, M.; Yang, J.; Shi, C.; Lv, J.; Feng, Y.; Zhang, W. Surface tailoring for selective endothelialization and platelet inhibition via a combination of SI-ATRP and click chemistry using Cys-Al-Gly-peptide. *Acta Biomater.* **2015**, *20*, 69–81. [CrossRef] [PubMed]

18. Yang, J.; Lv, J.; Gao, B.; Zhang, L.; Yang, D.; Shi, C.; Guo, J.; Li, W.; Feng, Y. Modification of polycarbonateurethane surface with poly(ethylene glycol) monoacrylate and phosphorylcholine glyceraldehyde for anti-platelet adhesion. *Front. Chem. Sci. Eng.* **2014**, *8*, 188–196. [CrossRef]

19. Shi, C.; Yuan, W.; Khan, M.; Li, Q.; Feng, Y.; Yao, F.; Zhang, W. Hydrophilic PCU scaffolds prepared by grafting PEGMA and immobilizing gelatin to enhance cell adhesion and proliferation. *Mater. Sci. Eng. C* **2015**, *50*, 201–209. [CrossRef] [PubMed]

20. Rujitanaroj, P.O.; Aid-Launais, R.; Chew, S.Y.; Le Visage, C. Polysaccharide electrospun fibers with sulfated poly(fucose) promote endothelial cell migration and VEGF-mediated angiogenesis. *Biomater. Sci.* **2014**, *2*, 843–852. [CrossRef]

21. Vatankhah, E.; Semnani, D.; Prabhakaran, M.P.; Tadayon, M.; Razavi, S.; Ramakrishna, S. Artificial neural network for modeling the elastic modulus of electrospun polycaprolactone/gelatin scaffolds. *Acta Biomater.* **2014**, *10*, 709–721. [CrossRef] [PubMed]

22. Jia, L.; Prabhakaran, M.P.; Qin, X.; Kai, D.; Ramakrishna, S. Biocompatibility evaluation of protein-incorporated electrospun polyurethane-based scaffolds with smooth muscle cells for vascular tissue engineering. *J. Mater. Sci.* **2013**, *48*, 5113–5124. [CrossRef]

23. Wang, G.; Hu, X.; Lin, W.; Dong, C.; Wu, H. Electrospun PLGA-silk fibroin-collagen nanofibrous scaffolds for nerve tissue engineering. *In Vitro Cell. Dev. Biol. Anim.* **2011**, *47*, 234–240. [CrossRef] [PubMed]

24. Chen, J.P.; Su, C.H. Surface modification of electrospun PLLA nanofibers by plasma treatment and cationized gelatin immobilization for cartilage tissue engineering. *Acta Biomater.* **2011**, *7*, 234–243. [CrossRef] [PubMed]

25. Wang, H.; Feng, Y.; Yang, J.; Guo, J.; Zhang, W. Targeting REDV peptide functionalized polycationic gene carrier for enhancing the transfection and migration capability of human endothelial cells. *J. Mater. Chem. B* **2015**, *3*, 3379–3391. [CrossRef]

26. Aghdam, R.M.; Najarian, S.; Shakhesi, S.; Khanlari, S.; Shaabani, K.; Sharifi, S. Investigating the effect of PGA on physical and mechanical properties of electrospun PCL/PGA blend nanofibers. *J. Appl. Polym. Sci.* **2012**, *124*, 123–131. [CrossRef]

27. Hao, X.; Li, Q.; Lv, J.; Yu, L.; Ren, X.; Zhang, L.; Feng, Y.; Zhang, W. CREDVW-linked polymeric micelles as a targeting gene transfer vector for selective transfection and proliferation of endothelial cells. *ACS Appl. Mater. Interfaces* **2015**, *7*, 12128–12140. [CrossRef] [PubMed]

28. Ji, W.; Yang, F.; Seyednejad, H.; Chen, Z.; Hennink, W.E.; Anderson, J.M.; van den Beucken, J.; Jansen, J.A. Biocompatibility and degradation characteristics of PLGA-based electrospun nanofibrous scaffolds with nanoapatite incorporation. *Biomaterials* **2012**, *33*, 6604–6614. [CrossRef] [PubMed]

29. Meng, Z.X.; Li, H.F.; Sun, Z.Z.; Zheng, W.; Zheng, Y.F. Fabrication of mineralized electrospun PLGA and PLGA/gelatin nanofibers and their potential in bone tissue engineering. *Mater. Sci. Eng. C* **2013**, *33*, 699–706. [CrossRef] [PubMed]

30. Han, J.; Lazarovici, P.; Pomerantz, C.; Chen, X.; Wei, Y.; Lelkes, P.I. Co-electrospun blends of PLGA, gelatin, and elastin as potential nonthrombogenic scaffolds for vascular tissue engineering. *Biomacromolecules* **2011**, *12*, 399–408. [CrossRef] [PubMed]

31. Sofokleous, P.; Stride, E.; Edirisinghe, M. Preparation, characterization, and release of amoxicillin from electrospun fibrous wound dressing patches. *Pharm. Res.* **2013**, *30*, 1926–1938. [CrossRef] [PubMed]

32. Ren, X.; Feng, Y.; Guo, J.; Wang, H.; Li, Q.; Yang, J.; Hao, X.; Lv, J.; Ma, N.; Li, W. Surface modification and endothelialization of biomaterials as potential scaffolds for vascular tissue engineering applications. *Chem. Soc. Rev.* **2015**, *44*, 5680–5742. [CrossRef] [PubMed]

33. Feng, Y.; Lu, J.; Behl, M.; Lendlein, A. Progress in depsipeptide-based biomaterials. *Macromol. Biosci.* **2010**, *10*, 1008–1021. [CrossRef] [PubMed]

34. Feng, Y.; Behl, M.; Kelch, S.; Lendlein, A. Biodegradable multiblock copolymers based on oligodepsipeptides with shape-memory properties. *Macromol. Biosci.* **2009**, *9*, 45–54. [CrossRef] [PubMed]

35. Zhang, L.; Feng, Y.; Tian, H.; Shi, C.; Zhao, M.; Guo, J. Controlled release of doxorubicin from amphiphilic depsipeptide-PDO-PEG-based copolymer nanosized microspheres. *React. Funct. Polym.* **2013**, *73*, 1281–1289. [CrossRef]

36. Helder, J.; Kohn, F.E.; Sato, S.; van den Berg, J.W.; Feijen, J. Synthesis of poly[oxyethylidenecarbonylimino (2-oxoethylene)][poly(glycine-D,L-lactic acid)] by ring opening polymerization. *Die Makromol. Chem. Rapid Commun.* **1985**, *6*, 9–14. [CrossRef]

37. Feng, Y.; Guo, J. Biodegradable polydepsipeptides. *Int. J. Mol. Sci.* **2009**, *10*, 589–615. [CrossRef] [PubMed]

38. Abayasinghe, N.K.; Perera, K.P.U.; Thomas, C.; Daly, A.; Suresh, S.; Burg, K.; Harrison, G.M.; Smith, D.W. Amido-modified polylactide for potential tissue engineering applications. *J. Biomater. Sci. Polym. Ed.* **2004**, *15*, 595–606. [CrossRef] [PubMed]

39. Lou, X.; Detrembleur, C.; Jérôme, R. Novel aliphatic polyesters based on functional cyclic (di)esters. *Macromol. Rapid Commun.* **2003**, *24*, 161–172. [CrossRef]

40. Feng, Y.; Klee, D.; Keul, H.; Höcker, H. Lipase-catalyzed ring-opening polymerization of morpholine-2,5-dione derivatives: A novel route to the synthesis of poly(ester amide)s. *Macromol. Chem. Phys.* **2000**, *201*, 2670–2675. [CrossRef]

41. Feng, Y.; Klee, D.; Höcker, H. Lipase-catalyzed ring-opening polymerization of 6(*S*)-methyl-morpholine-2,5-dione. *J. Polym. Sci. A Polym. Chem.* **2005**, *43*, 3030–3039. [CrossRef]

42. Shi, C.; Yao, F.; Huang, J.; Han, G.; Li, Q.; Khan, M.; Feng, Y.; Zhang, W. Proliferation and migration of human vascular endothelial cells mediated by ZNF580 gene complexed with mPEG-*b*-P(MMD-*co*-GA)-*g*-PEI microparticles. *J. Mater. Chem. B* **2014**, *2*, 1825–1837. [CrossRef]

43. Hägglund, B.; Sandberg, G. Effect of L-alanine and some other amino acids on thymocyte proliferation *in vivo*. *Immunobiology* **1993**, *188*, 62–69. [CrossRef]

44. Mallakpour, S.; Soltanian, S.; Sabzalian, M.R. Studies on synthesis and *in vitro* biodegradability of novel optically active nanostructure poly(ester-imide)s containing L-phenylalanine and L-isoleucine linkages. *Colloid Polym. Sci.* **2011**, *289*, 93–100. [CrossRef]

45. Deshmukh, M.; Singh, Y.; Gunaseelan, S.; Gao, D.; Stein, S.; Sinko, P.J. Biodegradable poly(ethylene glycol) hydrogels based on a self-elimination degradation mechanism. *Biomaterials* **2010**, *31*, 6675–6684. [CrossRef] [PubMed]

46. Li, Q.; Shi, C.; Zhang, W.; Behl, M.; Lendlein, A.; Feng, Y. Nanoparticles complexed with gene vectors to promote proliferation of human vascular endothelial cells. *Adv. Healthc. Mater.* **2015**, *4*, 1225–1235. [CrossRef] [PubMed]

47. Zhang, L.; Feng, Y.; Tian, H.; Zhao, M.; Khan, M.; Guo, J. Amphiphilic depsipeptide-based block copolymers as nanocarriers for controlled release of ibuprofen with doxorubicin. *J. Polym. Sci. A Polym. Chem.* **2013**, *51*, 3213–3226. [CrossRef]

48. Lv, J.; Zhang, L.; Khan, M.; Ren, X.; Guo, J.; Feng, Y. Biodegradable depsipeptide-PDO-PEG-based block copolymer micelles as nanocarriers for controlled release of doxorubicin. *React. Funct. Polym.* **2014**, *82*, 89–97. [CrossRef]

49. Shi, C.; Yao, F.; Li, Q.; Khan, M.; Ren, X.; Feng, Y.; Huang, J.; Zhang, W. Regulation of the endothelialization by human vascular endothelial cells by *ZNF580* gene complexed with biodegradable microparticles. *Biomaterials* **2014**, *35*, 7133–7145. [CrossRef] [PubMed]

50. Feng, Y.; Chen, C.; Zhang, L.; Tian, H.; Yuan, W. Synthesis and characterization of novel copolymers based on 3(*S*)-methyl-morpholine-2,5-dione. *Trans. Tianjin Univ.* **2012**, *18*, 315–319. [CrossRef]

51. Yao, J.; Pantano, M.F.; Pugno, N.M.; Bastiaansen, C.W.; Peijs, T. High-performance electrospun co-polyimide nanofibers. *Polymer* **2015**, *76*, 105–112. [CrossRef]

52. He, W.; Yong, T.; Teo, W.E.; Ma, Z.; Ramakrishna, S. Fabrication and endothelialization of collagen-blended biodegradable polymer nanofibers: Potential vascular graft for blood vessel tissue engineering. *Tissue Eng.* **2005**, *11*, 1574–1588. [CrossRef] [PubMed]

53. Luu, Y.; Kim, K.; Hsiao, B.; Chu, B.; Hadjiargyrou, M. Development of a nanostructured DNA delivery scaffold via electrospinning of PLGA and PLA-PEG block copolymers. *J. Control. Release* **2003**, *89*, 341–353. [CrossRef]

54. Ranjbar-Mohammadi, M.; Zamani, M.; Prabhakaran, M.; Bahrami, S.H.; Ramakrishna, S. Electrospinning of PLGA/gum tragacanth nanofibers containing tetracycline hydrochloride for periodontal regeneration. *Mater. Sci. Eng. C* **2016**, *58*, 521–531. [CrossRef] [PubMed]

55. Ravichandran, R.; Venugopal, J.R.; Sundarrajan, S.; Mukherjee, S.; Ramakrishna, S. Precipitation of nanohydroxyapatite on PLLA/PBLG/collagen nanofibrous structures for the differentiation of adipose derived stem cells to osteogenic lineage. *Biomaterials* **2012**, *33*, 846–855. [CrossRef] [PubMed]

56. Zhang, E.; Zhu, C.; Yang, J.; Sun, H.; Zhang, X.; Li, S.; Wang, Y.; Sun, L.; Yao, F. Electrospun PDLLA/PLGA composite membranes for potential application in guided tissue regeneration. *Mater. Sci. Eng. C* **2016**, *58*, 278–285. [CrossRef] [PubMed]